

1 **SUPPLEMENTARY DATA**

2

3 Table T-1. sampling locations

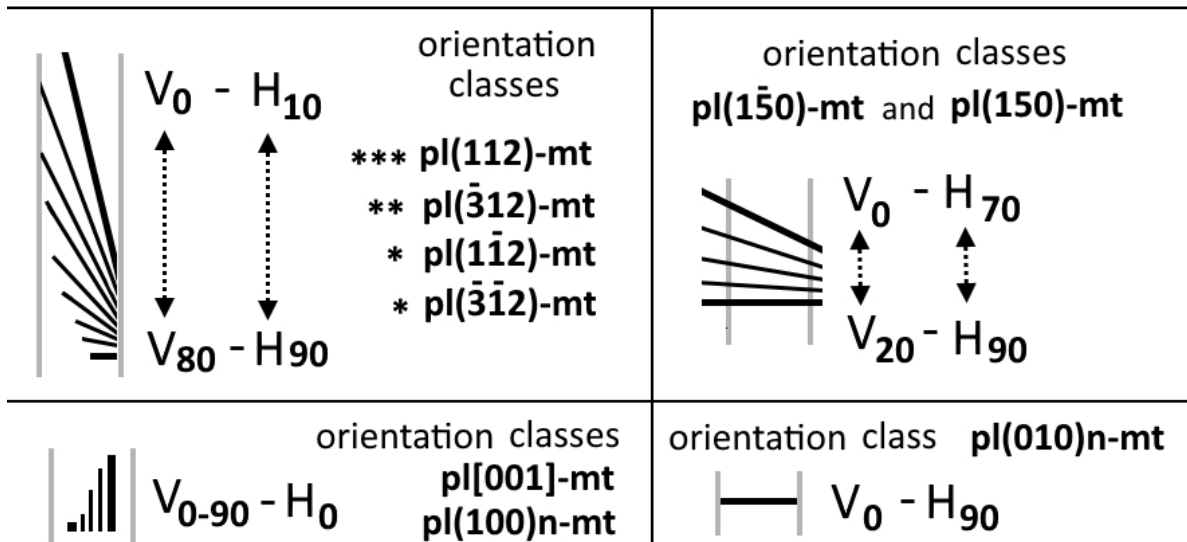
dredge number	latitude, deg. N*	longitude, deg. W*	depth, mbsl*	geological structure
L2612	10.708	41.570	5195	Vema Transform Fault
L30-277	13.027	44.869	4089	OCC 13°N
L32-101	13.570	44.916	3407	OCC 13°30'N
1514	12.593	44.516	4116	Ashadze complex
1491	12.990	44.906	3300	Ashadze complex

4 \*dredge track start points

5 OCC – oceanic core complex (see text).

6

**(010)-girdle**



7

8 **Figure S-I.** Determination of the orientation classes in petrographic thin sections.

9 In cuts, where the albite twin boundaries are approximately perpendicular to the thin section  
 10 plane the albite twin boundaries are very thin. In these sections the identification the different  
 11 inclusion orientation classes that play a role in the formation of magnetic anisotropy is possible  
 12 based on the angular relations of the magnetite needles with the plane of the albite twin boundary  
 13 (vertical angle) and with the plane of the thin section cut (horizontal angle).

14 The needle-shaped magnetite micro-inclusions are represented by the black lines. The  
 15 length of the lines is inversely proportional to the tilt of the inclusions relative to the surface of

16 the thin section. The cut with the albite twin boundary which is perpendicular to the thin section  
17 is represented by the vertical gray lines:

18 1. For the inclusions of pl(112)-mt, pl(-312)-mt, pl(1-12)-mt and pl(-3-12)-mt classes, the  
19 horizontal angle  $H=10^\circ$ , when the vertical angle  $V=0^\circ$ , and the horizontal angle  $H=90^\circ$ , when the  
20 vertical angle  $V=80^\circ$ . All possible orientations lie between these two orientations: the vertical  
21 (V) angle changes from  $0^\circ$  to  $80^\circ$ , the horizontal angle (H) changes from  $10^\circ$  to  $90^\circ$  (dashed  
22 lines with arrows). The angles H and V have positive correlation. The number of stars indicates  
23 the relative abundance of the orientation class of the micro-inclusions. The micro-inclusions  
24 belong to the (010)-girdle.

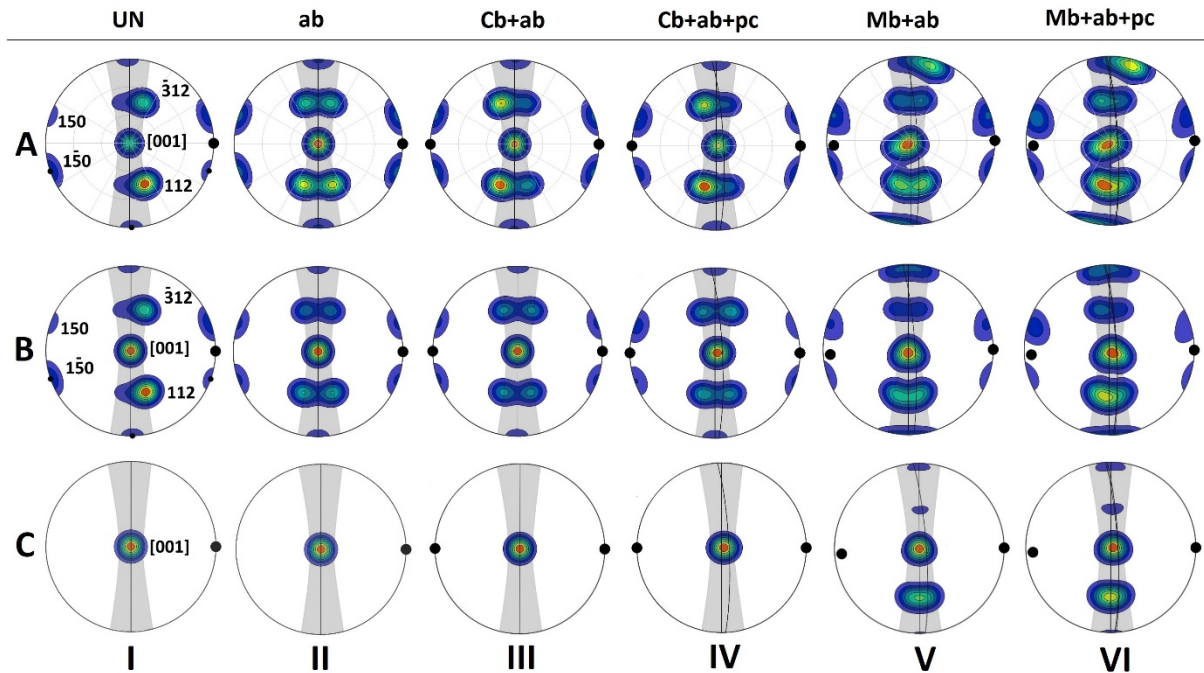
25 2. The pl(150)-mt and pl(1-50)-mt inclusions always are sub-horizontal with vertical angle (V)  
26 from  $0^\circ$  to  $20^\circ$ , and have a large horizontal angle (H) from  $70^\circ$  and  $90^\circ$  with the twin boundary.  
27 The angles H and V show positive correlation. The two types of the micro-inclusions often  
28 intersect the albite twin boundaries and are observed at about similar proportions.

29 3. The pl[001]-mt and pl(100)n-mt micro-inclusions are parallel to the albite twin boundaries  
30 ( $H=0^\circ$ ). They change vertical (V) angle from  $0^\circ$  to  $90^\circ$ . The pl[001]-mt class is more abundant  
31 than the pl(100)n-mt class. The micro-inclusions belong to the (010)-girdle.

32 4. The pl(010)n-mt micro-inclusions are rare in the plagioclase of oceanic gabbro. They are  
33 horizontal and perpendicular to albite twin boundaries ( $V=0$ ,  $H=90$ ).

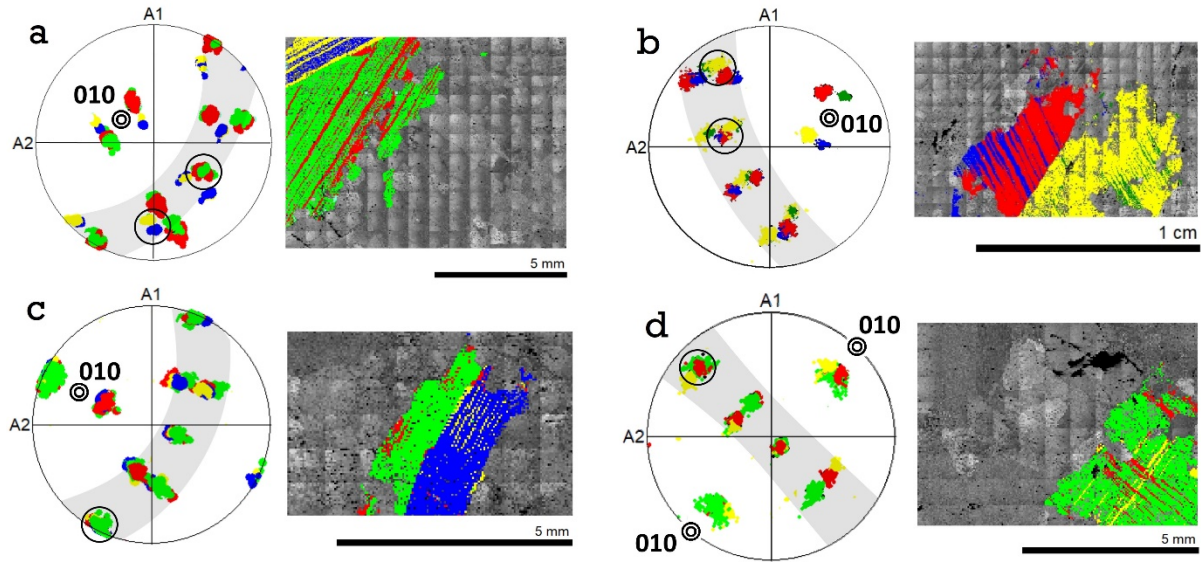
34 Note, the image does not reveal the mutual orientations between the micro-inclusions. The  
35 angles are rounded to nearest ten.

36



37  
38  
39  
40  
41  
42  
43  
44  
45  
46  
47  
48  
49  
50

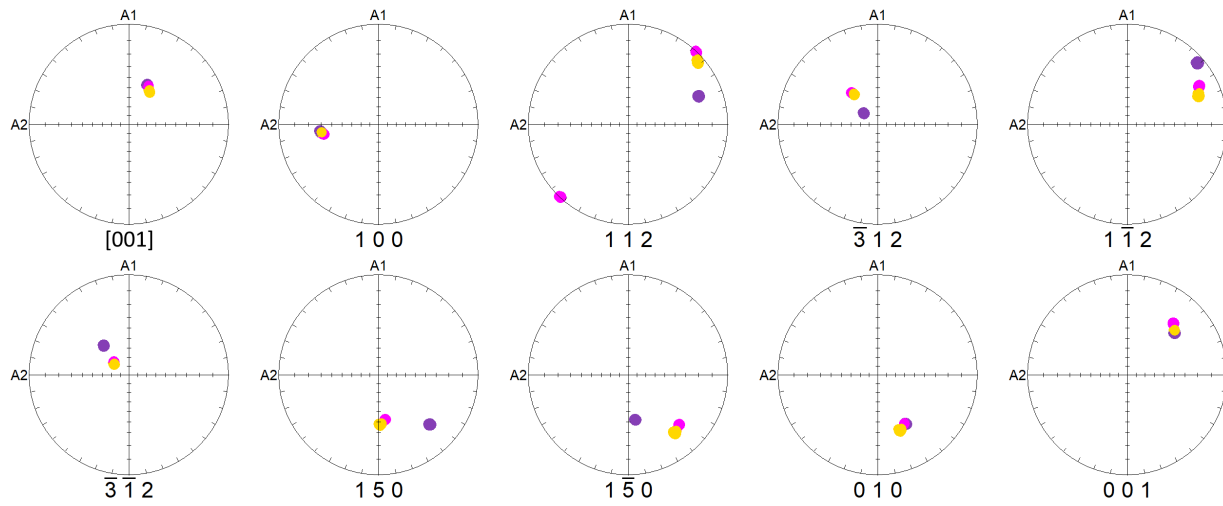
**Figure S-II.** Schematic plots of orientation distributions showing simulated statistical distributions (halfwidth 30 °) of the magnetite needle orientations in plagioclase with different combinations of twinning (Ab - Albite, p - pericline, Cb – Carlsbad, Mb – Manebach, UN - untwinned). In the first row (A) only the dominating “plane-normal” orientation class of magnetite micro-inclusions is considered. In the second row (B), both, the “plane-normal” and the pl[001]-mt orientation classes are considered. In the third row (C) only the pl[001]-mt orientation class is considered. The proportion of the inclusions pertaining to the different orientation classes are shown in Table 1. The 30°-girdle parallel to the pl(010) plane (gray areas) comprises the micro-inclusions oriented perpendicular to the pl(112), pl( $\bar{3}12$ ), pl(100), pl( $1\bar{1}2$ ), pl( $\bar{3}\bar{1}2$ ), and along the pl[001] direction.



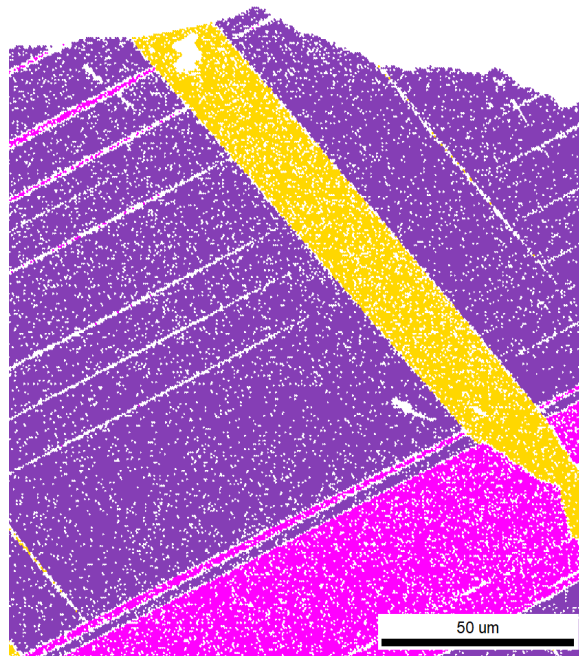
51  
 52 **Figure S-III.** Pole figures showing the poles of the plagioclase planes (EBSD data), which  
 53 correspond to the elongation directions of the needle-shaped magnetite micro-inclusions of all  
 54 eight orientation classes and orientation maps corresponding to these orientations. The  
 55 plagioclase grains are twinned after the Manebach and Albite laws (a, b); Carlsbad and albite  
 56 laws (c); and Pericline and Albite laws (d). The "30-degree girdles" containing the elongation  
 57 directions of the majority of the oriented micro-inclusions are shaded in gray. The double circles  
 58 indicate the poles of the pl(010) plane.  
 59

60

61



62

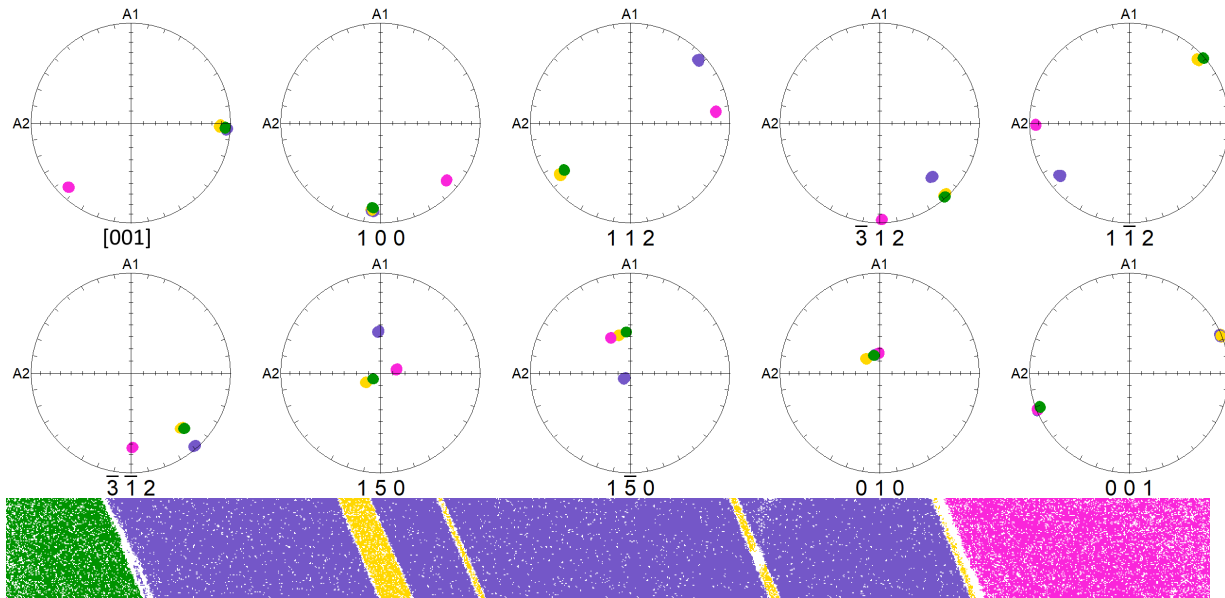


63

64

65

a.



66

67

68

69

b.

70 **Figure S-IV.** Stereographic projections (upper hemisphere) showing the poles of plagioclase  
 71 lattice planes and directions including those corresponding to the elongation directions of the  
 72 magnetite inclusions and planes, and orientation maps corresponding to these projections. (a)  
 73 Sample 1514-17. The plagioclase grain is twinned after the Albite law (highlighted by purple and  
 74 magenta colors) and by the Pericline law (yellow). See also Figure 9 (a- c). (b) Sample 1491-10.  
 75 The plagioclase grain is twinned after the Manebach law. One Manebach twin is highlighted by  
 76 magenta color, another one is twinned after the Pericline law (purple and yellow colors), and the  
 77 Pericline + Albite law (green). See also Figure 9 (d- f).

78